Avian coronary endothelium is a mosaic of sinus venosus- and ventricle-derived endothelial cells in a region-specific manner

Avian coronary endothelium is a mosaic of sinus venosus- and ventricle-derived endothelial cells in a region-specific manner

Tatsuya Kamimura, Toshiyuki Yamagishi, Yuji Nakajima

Tatsuya Kamimura, Toshiyuki Yamagishi, Yuji Nakajima. (2018). Avian coronary endothelium is a mosaic of sinus venosus- and ventricle-derived endothelial cells in a region-specific manner. *Development, Growth & Differentiation*. 60(2),97-111

Avian coronary endothelium is a mosaic of sinus venosus- and ventricle-derived endothelial cells in a region-specific manner

Tatsuya Kamimura, Toshiyuki Yamagishi, Yuji Nakajima

Avian coronary endothelium is a mosaic of sinus venosus- and ventricle-derived endothelial cells in a region-specific manner

Short title: Origin of coronary endothelial cells

Tatsuya Kamimura, Toshiyuki Yamagishi, Yuji Nakajima*

Department of Anatomy and Cell Biology, Graduate School of Medicine, Osaka City University, Osaka, 545-8585 Japan

*Corresponding author:

Yuji Nakajima, Department of Anatomy and Cell Biology, Graduate School of Medicine, Osaka City University, 1-4-3 Asahimachi, Abenoku, Osaka, 545-8585 Japan

E-mail: yuji@med.osaka-cu.ac.jp (YN)

Tel: +81-6-6645-3705

Fax: +81-6-6646-3603

Abstract

The origin of coronary endothelial cells (ECs) has been investigated in avian species, and the results showed that the coronary ECs are thought to originate from the proepicardial organ (PEO) and developing epicardium. Genetic approaches in mouse models showed that the major source of coronary ECs is the sinus venosus endothelium or ventricular endocardium. To clarify and reconcile the differences between avian and mouse species, we examined the source of coronary ECs in avian embryonic hearts. Using an enhanced green fluorescent protein-Tol2 system and fluorescent dye labeling, four types of quail-chick chimeras were made and quail-specific endothelial marker (QH1) immunohistochemistry was performed. The developing PEO consisted of at least two cellular populations, one was sinus venosus endothelium-derived inner cells and the other was surface mesothelium-derived cells. The majority of ECs in the coronary stems, ventricular free wall, and dorsal ventricular septum originated from the sinus venosus endothelium. The ventricular endocardium contributed mainly to the septal artery and a few cells to the coronary stems. Surface mesothelial cells of the PEO differentiated mainly into a smooth muscle phenotype, but a few differentiated into ECs. In avian species, the coronary endothelium had a heterogeneous origin in a region-

specific manner, and the sources of ECs were basically the same as those observed in mice.

Key words: avian heart, coronary artery development, origin, endocardium, EGFP-Tol2

Introduction

Coronary vessels function to supply oxygen and nutrients to the cardiac muscle to maintain the heart beat. During heart development in the early embryonic stages, oxygen and nutrients are supplied to the myocardium by diffusion through the inner endocardium. At the onset of the fetal stage, endothelial cells (ECs) from the peritruncal endothelial plexus invade into the aortic sinuses to form coronary stems, thereafter coronary circulation starts and continues throughout life (Ando *et al.* 2004). Disruption of coronary circulation causes ischemic heart disease including angina pectoris and myocardial infarction. Improved understanding of the developmental biology of coronary vessels is necessary to develop therapeutic strategies for revascularization of the ischemic heart.

The coronary artery consists of three distinct layers, the tunica interna, tunica media, and tunica externa. It is well accepted that not only vascular smooth muscle cells of the tunica media but also interstitial cells of the tunica externa originate from the

52 developing epicardium. The developing epicardium is a derivative of the proepicardial
53 organ (PEO), which is a cauliflower-shaped protrusion extending from the mesothelial
54 layer covering the ventral surface of the sinus venosus (SV) (Hiruma *et al*. 1989;
55 Mikawa & Fischman 1992; Mikawa & Gourdie 1996; Dettman *et al*. 1998). The
56 developing epicardium undergoes epithelial-to-mesenchymal transition to seed
57 subepicardial mesenchymal cells, which later give rise to vascular smooth muscle and
58 interstitial cells (Mikawa & Gourdie 1996; Dettman *et al*. 1998). Genetic cell-tracing
59 experiments in mouse embryos showed that the major source of coronary ECs is the SV
60 endothelium and/or ventricular endocardium (Red-Horse *et al*. 2010; Wu *et al*. 2012;
61 Tian *et al*. 2013; Chen *et al*. 2014; Tian *et al*. 2015; Zhang *et al*. 2016). In the neonatal
62 mouse heart, ventricular endocardium contributes to form the subendocardial coronary
63 vasculatures (Tian *et al*. 2015). In avian hearts, retrovirus cell-tracing, quail-chick
64 chimera, and dye-marking experiments showed that cells from the PEO differentiate
65 into the epicardium, vascular smooth muscle, and coronary endothelium (Mikawa &
66 Fischman 1992; Männer 1999; Pérez-Pomares *et al*. 2002). The discrepancy of the
67 origin of coronary ECs between mouse and avian species as well as among mouse
68 models is an unresolved issue.

69 The PEO is a transient tissue consisting of surface mesothelium and inner

70 mesenchymal-like populations. Matured PEO adheres to the dorsal surface of the
71 atrioventricular groove and spreads over the heart in a dorsal-to-ventral direction to
72 generate the epicardium (Hiruma *et al*. 1989; Nakajima & Imanaka-Yoshida 2013). In
73 the mouse PEO, a *Scleraxis*-/*Semaphorin3D*-expressing population gives rise to
74 coronary ECs, whereas *Tbx18*/*Wt1*-positive surface mesothelial cells provide the
75 epicardium, vascular smooth muscle, and myocardial interstitial cells (Katz *et al*. 2012).
76 In the avian PEO, hematopoietic- and endothelial-marker positive cells are observed just
77 before attaching to the ventricle (Poelmann *et al*. 1993; Kattan *et al*. 2004; Guadix *et al*.
78 2006; Niderla-Bielinska *et al*. 2015). The origin and nature of the inner hemangioblast-
79 like population remain uncertain.

80 In the present study, using enhanced green fluorescent protein (EGFP)-Tol2 and
81 fluorescent dye labeling in combination with quail-chick chimera, we examined the
82 origin of coronary ECs and the relative contributions of their distinct sources for
83 coronary vessels. The results showed that cells from the SV endothelium migrated into
84 the PEO, subepicardial space, and ventricular wall, and contributed to coronary vessels
85 in the ventricular free wall including coronary stems. Ventricular endocardium
86 contributed mainly to the septal coronary vessels. The surface mesothelial cells of the
87 PEO differentiated into coronary smooth muscle cells but a few of them also

contributed to the coronary endothelium.

Materials and methods

Chick and quail embryos

Fertilized eggs (chick [*Gallus gallus*], Shiroyama Farm, Kanagawa, Japan; quail [*Coturnix japonica*], Quail Cosmos, Aichi, Japan) were incubated at 37°C and 60% humidity. After an appropriate incubation period, 4 mL (1 mL in quail) of egg albumin was removed and a fenestration (1.5×2 cm) (1×1 cm in quail) was made, followed by injection of 10% carbon ink/Tyrode's solution into the yolk sac beneath the embryo, and staged in accordance with Hamburger and Hamilton (Hamburger & Hamilton 1951). Embryos were subjected to EGFP-Tol2 or dye labeling as well as chimera generation. Animal handling and procedures were approved by the Osaka City University Animal Care and Use Committee, as set forth in the NIH Guide for the Care and Use of Laboratory Animals (Eighth Edition).

Preparation of EGFP-Tol2 transfection mixture

To label the target cells across the cell cycles, transfection of the EGFP-Tol2 system was attempted. The transfection mixture was prepared using Lipofectamine

106 2000 (Thermo Fisher Scientific Inc., MA, USA) in accordance with the manufacturer's
107 instructions with a minor modifications
108 (https://www.thermofisher.com/jp/ja/home/references/protocols/cell-
109 culture/transfection-protocol/lipofectamine-2000.html#procedure). Lipofectamine 2000
110 was diluted with Opti-MEM I (0.8 μL/μL, Thermo Fisher Scientific Inc.) and incubated
111 for 5 minutes at room temperature. The same amount of CAGGS-transposase
112 (pCAGGS-T2TP) (kindly donated by Dr Kawakami, National Institute of Genetics) and
113 Tol2-flanked CAGGS-EGFP (pT2K-CAGGS-EGFP) (kindly donated by Dr Takahashi,
114 Kyoto University) (Sato *et al*. 2007) were diluted with Opti-MEM I (0.28 μg/μL). The
115 same amounts of diluted Lipofectamine 2000 and DNA were mixed gently and
116 incubated for 20 minutes at room temperature. The resulting transfection mixture, which
117 contained pCAGGS-T2TP (0.14 μg/μL), pT2K-CAGGS-EGFP (0.14 μg/μL) and
118 Lipofectamine 2000 (0.4 μL/μL) (0.075%), was used for labeling experiments.
119

120 Fluorescent labeling *in ovo*

121 To label the SV ECs, 2 μL of acetylated low-density lipoprotein labeled with 1,1'-
122 dioctadecyl-3,3,3',3-tetramethylindo-carbocyanine perchlorate (DiI-LDL; 100 μg/mL in
123 0.05% fast green/phosphate-buffered saline [PBS]; Biomedical Technologies Inc., MA,

124 USA) was slowly injected into the peripheral vitelline vein of stage 14–15 embryos
125 using a sharpened pulled-glass needle (10–20 μm in external diameter) equipped with a
126 pressure injector (NARISHIGE, Tokyo, Japan). To label the surface mesothelial cells of
127 the PEO, 2 μL of 5- and 6-carbosyfluorescein diacetate succinimidyl ester (CFSE; 100
128 μmol/L in Tyrode's solution, Bioquest, CA, USA) (Kruithof *et al*. 2006) or 0.1–1 μL of
129 EGFP-Tol2 transfection mixture was slowly microinjected into the pericardial cavity of
130 stage 13–14 embryos using the pressure injector. To label the chick ventricular
131 endocardium or quail SV endothelium, 0.1–0.2 μL of EGFP-Tol2 transfection mixture
132 was slowly microinjected into the ventricle, atrium, or SV of cold-induced arrested
133 hearts at stage 12. Embryos were left for 1 hour at room temperature. After an additional
134 incubation period at 37°C, embryos were subjected to quail-chick chimera or organ
135 culture. Fluorescently labeled target cells (ECs and mesothelial cells) and the labeling
136 efficiency of EFGP-Tol2 system were shown in Fig. S1.
137

138 Quail-chick chimera

139 Four types of quail-chick chimera were prepared in accordance with a modified
140 method described by Männer (Fig. 1) (Männer 1999). To define the cranio-caudal
141 orientation of the PEO, a small long pentagonal-shaped eggshell membrane was

142 inserted into the stage 16–17 quail SV posterior to the PEO. SV with the PEO, and
143 eggshell membrane were carefully extirpated and transplanted orthotopically into the
144 host chick embryo. To avoid contamination of host SV ECs and PEO cells into the
145 chimeric heart, the host chick PEO was cauterized using a small vessel cauterizer before
146 transplantation (FST Inc., CA, USA). To trace the ECs of SV, stage 16–17 quail SV with
147 the PEO, in which ECs had been labeled with EGFP-Tol2 or DiI-LDL at stage 14, was
148 orthotopically transplanted into the PEO-cauterized host chick embryos at stage 17
149 (n=26, Fig. 1A). To trace the surface mesothelial cells of the PEO, stage 16–17 quail SV
150 with PEO, in which mesothelial cells had been labeled with EGFP-Tol2 or CFSE at
151 stage 12–13, was orthotopically transplanted into the PEO-cauterized host chick
152 embryos at stage 17 (n=22, Fig. 1B). To trace both surface mesothelial cells of the PEO
153 and ECs of the SV, stage 16–17 quail SV with the PEO, in which mesothelial cells had
154 been labeled with CFSE at stage 12–13, followed by reincubation, and SV labeling with
155 DiI-LDL at stage 14, was orthotopically transplanted into PEO-cauterized host chick
156 embryos at stage 17 (n=7, Fig. 1C). To trace the ventricular endocardium, stage 16–17
157 unlabeled quail SV with the PEO was orthotopically transplanted into PEO-cauterized
158 host chick hearts, in which the endocardium had been transfected with EGFP-Tol2 at
159 stage 12 (n=3, Fig. 1D). Number of chimeric hearts examined was summarized in Table

S1. There was no obvious cardiac anomaly except an adherent transplanted tissue on the dorsal surface of the atrioventricular region. We reported previously that PEO-deleted embryos die before stage 31 because of defective epicardium/coronary vessels and thin myocardium; therefore, coronary vessels observed in the chimeric heart mainly originated from the transplanted SV with the PEO (Takahashi *et al*. 2014).

Organ culture

SV with the PEO or PEO alone was prepared from stage 16–17 chick or quail embryos, in which SV endothelial cells or surface mesothelial cells were labeled with fluorescent dye as described above, were resected and cultured on an 8-well chamber slide (Thermo Fisher Scientific, MA, USA) supplemented with 200 μL of serum-free medium (75% Dulbecco's modified Eagle's medium [DMEM], 25% McCoy's medium, 10^{-7} mol/L dexamethasone, and penicillin-streptomycin, Sigma-Aldrich, MO, USA) (Yanagawa *et al*. 2011). After 48–96 hours in culture, cultures were fixed with 4% paraformaldehyde in PBS and subjected to immunohistochemistry.

Immunohistochemistry

Embryos or hearts were fixed in 4% paraformaldehyde in PBS for 30 minutes at

178 room temperature (for anti-WT1 staining) or 3 hours at 4°C (for other antibodies). After
179 extensive washing in PBS, samples were equilibrated in graded series of sucrose in PBS
180 (7%, 15%, 20% W/V) and embedded in optimum cutting temperature (OCT) compound
181 (Sakura, Tokyo, Japan) and frozen in liquid nitrogen. Frozen sections were cut using a
182 cryostat and mounted on slides. After being rinsed in PBS, sections were blocked with
183 1% bovine serum albumin (BSA)/PBS for 1 hour at room temperature, incubated with a
184 primary antibody for 2 hours at room temperature, rinsed with PBS, and incubated with
185 a secondary antibody for 2 hours at room temperature followed by nuclei staining with
186 4’,6-diamino-2-phenylindole dehydrochloride (DAPI) for 20 minutes. After washing in
187 PBS, samples were mounted and observed using a confocal laser microscope (Leica,
188 Wetzlar, Germany) or conventional fluorescence microscope equipped with cooled CCD
189 camera (Olympus, Tokyo, Japan).
190 Cultures were drained of medium, rinsed with PBS, and fixed with 4%
191 paraformaldehyde/PBS for 30 minutes at room temperature. After washing with PBS,
192 samples were blocked with 1% BSA/PBS containing 0.1% Triton X-100 (PBST) for 1
193 hour and incubated with a primary antibody for 2 hours at room temperature. Samples
194 were rinsed with PBS, incubated with a secondary antibody, and the nuclei stained with
195 DAPI. After washing, the samples were mounted in mounting medium and observed.

196 Using a Fluo Render (University of Utah, UT, USA), confocal images were stacked in
197 the z-axis direction and cross-sectional images were reconstructed.
198

199 Antibodies

200 The following primary antibodies were used: mouse monoclonal anti-quail-
201 specific endothelial marker QH1 (supernatant, 20×, Developmental Studies Hybridoma
202 Bank, University of Iowa, IA, USA), anti-WT1 (rabbit polyclonal, SC192, 100×, Santa
203 Cruz, Dallas, TX, USA), anti-smooth α-muscle actin (SMA, mouse monoclonal, clone
204 1A4, 500×, Sigma-Aldrich, MO, USA), anti-SM22α (rabbit serum, 200×, kindly
205 donated Dr Kobayashi, Kagawa University, Kagawa, Japan) (Shishibori *et al*. 1996),
206 and anti-calponin (mouse monoclonal, clone CP93, 150×, Sigma-Aldrich). Secondary
207 antibodies were: TRITC-conjugated goat anti-mouse IgG1 (cat #1070-03, 100×,
208 Southern Biotech, AL, USA), TRITC-conjugated goat anti-mouseIgG2a (cat #1080-03,
209 100×, Southern Biotech), Alexa Fluoro 405-conjugated goat anti-mouse IgG (cat#
210 ab175661, 500×, Abcam, Cambridge, UK), TRITC-conjugated donkey anti-rabbit IgG
211 (cat #AP182R, 100×, Millipore, Darmstadt, Germany), FITC-conjugated donkey anti-
212 rabbit IgG (cat #AP182F, 100×, Millipore), and FITC-conjugated donkey anti-mouse
213 IgG (cat #AP192F, 100×, Millipore).

Counting labeled cells and statistical analysis

Using an ImageJ (NIH), number of cells of interest (maker-positive, marker + EGFP [or fluorescent dye]-positive, EGFP [or fluorescent dye]-positive cells) was manually counted in histological images which were photographed under a 20× (or 40×) objective lens. Percentage of cells of interest in a certain cellular population was calculated. In stage 35 (E9 [embryonic day 9]) coronary artery, percentages of QH1-positive, EGFP-positive, and unlabeled cells were calculated in endothelial lining (more than 100 μm in length). Statistical analysis was performed by non-parametric Mann-Whitney *U* test and Bonferroni correction was used for multiple comparison. The significance level was set at <5%.

Results

The PEO consists of at least two cellular populations

At first we examined whether ECs of the SV contributed to the cellular population of the developing PEO. ECs in stage 14–15 chick embryos were labeled with DiI-LDL that had been injected via the peripheral vitelline vein to avoid mesothelial labeling. The embryos were reincubated and the PEO was inspected as to whether it

232 contained DiI-LDL-positive cells at stage 19. As shown in Fig. 2, DiI-LDL-positive- but
233 WT1-negative cells were observed in the PEO core-mesenchyme (white arrowheads in
234 Fig. 2A). In histological sections, 76 ± 12% of the core-mesenchymal cells had DiI-
235 LDL (Fig. S2). Mesothelial cells of the PEO, which expressed WT1, were unlabeled
236 with DiI-LDL (yellow arrowheads in Fig. 2A). Similar experiments using quail embryos
237 showed that both DiI-LDL- and QH1-positive cells were observed in the PEO (Fig.
238 S1A). We next examined the distribution of mesothelial-derived cells in the PEO.
239 Mesothelial cells of the pericardial cavity were labeled with CFSE at stage 13, at which
240 point mesothelial protrusion began to take place, then embryos were reincubated, and
241 the distribution of CFSE-positive cells in the PEO was examined at stage 16–17. CFSE-
242 labeled cells, which expressed high levels of WT1, were distributed on the surface of
243 the PEO and its subjacent region (yellow arrowheads in Fig. 2B). CFSE-negative/WT1-
244 negative cells were observed within the PEO (white arrowheads in Fig. 2B). These
245 results suggested that the PEO consisted of at least two cellular populations, one
246 comprising SV endothelium-derived cells and the other mesothelium-derived cells.
247

248 SV-derived ECs contribute to coronary vessels in the
249 ventricular free wall

To investigate whether SV-derived ECs contributed to coronary vessels, quail PEOs with SV, in which the ECs had been labeled with EGFP-Tol2 or DiI-LDL, was orthotopically transplanted into PEO-cauterized host chick embryos (Fig. 1A). After reincubation, the hearts of chimeric embryos were subjected to anti-QH1 (ECs) or anti-smooth muscle α-actin (SMA) immunohistochemistry. Coronary vessels with SMA-positive tunica media are identified as the coronary artery before stage 39 (E 13) (Vrancken Peeters *et al*. 1997). In stage 23 (E4) hearts, QH1-positive cells, some of which had EGFP, were observed in the subepicardial space and ventricular myocardium of the dorsal atrioventricular and ventricular regions (arrowheads in Fig. 3A). At stage 27–29 (E5–6), QH1-positive cells, some of which had EGFP, showed a strand-like structure, and these vessel-like structures were found in the subepicardial space and myocardium of the atrioventricular canal and ventricular free wall (arrowheads in Fig. 3B, C). At stage 31–34 (E7–8), coronary arteries (stems) connected with the aortic sinuses. QH1- and/or EGFP-positive cells were found in ECs of both the coronary artery stem (arrowheads in Fig. 3D) and cardiac vein (arrows in Fig. 3E). Coronary vessels develop closely associated with cardiac lymphatics, however PEO does not contribute to lymphangioblasts (Wilting *et al*. 2007). Observations suggested that quail SV ECs contributed to coronary ECs in the ventricular free wall including the coronary

artery stem and cardiac vein in the host chick heart.

Cultured SV ECs migrate through the PEO and maintain endothelial character

We next investigated whether ECs of SV were capable of migrating through the PEO and differentiating into ECs in culture. PEOs with SV, in which ECs had been labeled with DiI-LDL, were cultured for 24–96 hours and stained with the anti-QH1 antibody. QH1-positive cells migrated through the PEO and expanded on the culture dish (Fig. 4A–C). High magnification images showed that these migrating QH1-positive cells contained DiI-LDL (arrowheads in Fig. 4D–F), indicating that SV ECs were capable of migrating through the PEO to expand on the culture dish. After 48 hours in culture, DiI-LDL- and QH1-positive cells showed a mesenchymal appearance with cellular processes (Fig. 4G–I), and 37 ± 2% of DiI-LDL-positive cells was stained with QH1 (Fig. 4M). After 72–96 hours in culture, these cells showed a cobblestone appearance (Fig. 4J–L), and 79 ± 3% of DiI-LDL-positive cells expressed QH1 after 96 hours (Fig. 4M). These results suggested that ECs migrating from the SV through the PEO maintained their endothelial nature/lineage, but some of the migrating SV-derived cells were unlabeled with QH1 at the beginning of/during migration.

Surface mesothelial cells of the PEO contribute to the coronary smooth muscle but few of them to ECs

To examine whether PEO mesothelial cells contributed to coronary ECs, quail PEOs, in which mesothelial surface cells had been labeled with EGFP-Tol2 or CFSE, was transplanted orthotopically into PEO-cauterized host chick embryos (Fig. 1B). The chimeric embryos were reincubated and heart sections were stained with an anti-QH1 antibody or anti-SMA antibody. In stage 23 (E4) chimeric hearts, EGFP-positive cells and QH1-positive cells were observed in the epicardium/subepicardial layer of the dorsal atrioventricular groove. Some of EGFP-positive cells had a QH1 epitope (arrowheads in Fig. 5A). In stage 29 (E6) hearts, EGFP-positive cells were observed in the epicardium/subepicardial layer at the atrioventricular groove (Fig. 5B), dorsal ventricular wall, and conotruncal base. Some EGFP-positive cells with a QH1 epitope were recruited into the QH1-positive vessel-like structures (arrowheads in Fig. 5B). In stage 34 (E8) hearts, EGFP-positive cells were observed in the epicardium, subepicardial, and myocardial layers (Fig. 5C, D). Many of these cells expressing SMA were incorporated into the SMA-positive smooth muscle layer of the coronary artery (arrows in Fig. 5C). Some EGFP/QH1-positive cells were incorporated in to the

304 coronary artery and cardiac vein (arrowheads in Fig. 5D). In tissue sections of stage 34
305 hearts, the percentage of SMA-positive cells in EGFP-positive cells was much greater
306 than that of QH1-positive cells (Fig. S3). These results suggested that most surface
307 mesothelial cells of the PEO differentiated into smooth muscle cells but some of them
308 also differentiated into ECs.
309

310 Cultured PEO mesothelial cells differentiate into cells with
311 smooth muscle markers but only a small population gained
312 endothelial character

313 We next examined whether mesothelial cells of the PEO were capable of
314 differentiating into ECs in culture. CFSE-labeled chick or quail PEOs (without SV)
315 were cultured for 24–72 hours and stained with an anti-QH1 antibody and/or antibodies
316 against smooth muscle antigens. Almost all the cells spread over the culture dish had
317 CFSE, and more than 80% of these cells expressed smooth muscle markers (SM22α,
318 SMA, calponin). On the other hand, approximately 5% of CFSE-positive cells were
319 positively stained with the QH1 antibody (Fig. 6). Some CFSE/QH1-positive cells
320 showed vessel-like strands (Fig. 6D–H), in which a luminal structure was detected using
321 z-stack confocal images (Fig. 6H–K). The results suggested that CFSE-positive surface

322 mesothelial cells of the PEO mainly differentiated into cells with smooth muscle
323 markers, but only a few of them had endothelial characteristics.
324

325 QH1-positive subepicardial cells originated from SV
326 endothelium

327 The above experiments suggested that SV ECs contributed to coronary
328 endothelium rather than surface mesothelial cells of the PEO. We next examined the
329 ratio of SV-derived cells (or PEO mesothelial-derived cells) in QH1-positive cells in a
330 region where the PEO adhered to the dorsal atrioventricular region. Quail PEO with SV,
331 in which ECs and surface mesothelial cells had been labeled with DiI-LDL and CFSE,
332 respectively, was orthotopically transplanted into PEO-cauterized chick embryo at stage
333 17 (Fig. 1C). In stage 24 (E4) hearts, CFSE-positive cells were distributed in the
334 epicardium and its subjacent region, whereas DiI-LDL-positive cells were observed in
335 the subepicardial and myocardial regions (Fig. 7A). QH1 staining showed that QH1-
336 positive cells with DiI-LDL (arrowheads in Fig. 7B) were more predominant than those
337 with CFSE (arrows in Fig. 7C). To examine the percentage of SV-derived or PEO-
338 mesothelial derived cells in QH1-positive cell, quail PEO with SV, in which ECs or
339 surface mesothelial cells had been labeled with fluorescent dye (Fig. 1A, B), was

transplanted. At stage 24 (E4), the percentage of DiI-LDL- or CFSE-positive cells in the QH1-positive cells were counted manually in tissue sections. The percentage of DiI-LDL-positive cells (44.5 ± 6.1%) in the QH1-stained cells was significantly higher than that of CFSE-positive cells (5.1 ± 0.9%) (P=0.0495, Mann-Whitney U test, Fig. 7D). Results suggested that the majority of QH1-positive cells in the region where the PEO attached to the ventricle originated from the SV endothelium.

Ventricular endocardium contributes to the septal artery

We next examined whether ventricular endocardium contributed to coronary vessels in the chick heart. Unlabeled quail PEO with SV was orthotopically transplanted into PEO-cauterized chick hearts, in which the endocardium had been transfected with EGFP-Tol2 (Fig. 1D). In stage 35 (E9) chimeric hearts, QH1-positive cells were distributed in a compact myocardial layer in the left and right ventricular free wall, whereas EGFP-positive cells were observed in the endocardial lining of the trabecular layer (Fig. 8A, B). In the ventricular septum, QH1-positive cells were densely distributed in the dorsal region adjoining the ventricular free wall (Fig. 8C), whereas QH1-positive cells were sparse and EGFP-positive cells were observed in the middle to ventral aspect of the septum (arrowheads in Fig. 8C2, 3). At this stage, we observed

358 well-developed coronary stems as well as the septal artery (major coronary artery
359 originating from the coronary stem in chick hearts) (Lindsay & Smith 1965), which had
360 an SMA-positive medial layer (Fig. 8D1, F1). The endothelium of these main coronary
361 arteries had both QH1-positive (quail SV origin, arrows in Fig. 8E, G) and EGFP-
362 positive ECs (chick ventricle origin, arrowheads in Fig. 8E, G). The percentages of
363 QH1- or EGFP-positive ECs in the coronary endothelium were calculated, in which the
364 vascular segment was more than 100 μm in histological sections (Fig. 9). The result
365 showed that 50–100% (mean 72%) of ECs in the coronary stems had QH1
366 immunoreactivity (SV derived cells) and the percentages of QH1-positive ECs were
367 significantly high in both right and left coronary stems. In the dorsal segment of the
368 septal artery 47% of ECs had QH1, whereas the rates were 14% in medial and 20% in
369 the ventral segments. Less than 20% of ECs contained detectable amounts of EGFP in
370 either the coronary stem or septal artery, and unlabeled ECs were predominant in the
371 medial and ventral septal arteries. The origin of unlabeled coronary ECs was uncertain;
372 however, the ventricular endocardium was a candidate for the source of unlabeled ECs
373 rather than the host SV/PEO, because the host PEO was cauterized and 90% of the
374 coronary ECs in the ventricular free wall were transplanted quail SV in origin (Fig. S4).
375 These observations suggested that SV ECs were the major source of coronary stem and

376 coronary vessels in the ventricular free wall, whereas the ventricular endocardium
377 contributed mainly to the ventricular septum. Schematic representations of the sources
378 of coronary ECs were shown in Fig. 10.
379

380 Discussion

381 PEO consists of at least two distinct tissue compartments in
382 origin

383 Our dye-labeling experiments showed that the mature PEO consisted of at least
384 two distinct cellular populations, which were CFSE-labeled surface mesothelial cells
385 highly expressing WT1, and DiI-LDL-labeled SV-derived inner mesenchymal-like
386 population. In the mouse PEO, there are three genetically distinct cellular
387 compartments, in which *Wt1/Tbx18*-, *Scleraxis*-, and *Semaphorin3D*-expressing cells
388 are identified (Katz *et al*. 2012). *Wt1*-positive surface PEO cells differentiate into
389 epicardium, smooth muscle cells, and interstitial cells. This cellular population is also
390 required to form the coronary arterio-venous connection (Cano *et al*. 2016). *Scleraxis*-
391 positive but *Wt1*-negative mesothelial cells are observed mainly in the surface of the
392 PEO and are competent to give rise to coronary ECs (Katz *et al*. 2012). *Semaphorin3D*-
393 positive cells, which are observed in the mesenchymal-like compartment of the mouse

394 PEO, differentiate not only into coronary ECs but also SV ECs (Katz *et al*. 2012). The
395 surface mesothelial cells in the mouse PEO are similar in nature to avian surface PEO
396 cells, which were capable of differentiating to smooth muscle cells and ECs *in vivo* and
397 *in vitro*. *Semaphorin3D*-positive core compartment in the mouse PEO appears to be
398 similar in nature to the WT1-negative inner population of the avian PEO. The origin of
399 the core mesenchymal population remains uncertain. Our dye-labeling experiment
400 suggests that the mesenchymal-like population in the PEO mainly originate from the SV
401 ECs, because significant amount of the inner cells were labeled with DiI-LDL, which
402 was injected into the peripheral vitelline vein, and SV ECs expressed an epithelial-
403 mesenchymal transition marker, Slug, at the onset of/during PEO protrusion (Fig. S2).
404 However, we could not rule out the possibility that the liver bud-derived ECs contribute
405 to the PEO in avian species (Cossette & Misra 2011), because there is no specific
406 marker to identify the liver bud-derived angioblasts. The PEO is a transient but
407 important structure because it provides epicardium, interstitial cells, and coronary
408 vessels to maintain myocardial growth and maturation (Gittenberger-de Groot *et al*.
409 2000; Pennisi *et al*. 2003; Takahashi *et al*. 2014). However, little is known about the
410 molecular and cellular mechanisms underlying the specification/determination and early
411 development of the PEO (Niderla-Bielinska *et al*. 2015). Our *in vivo* and *in vitro*

412 analyses clarified that the PEO consists of at least two cellular populations, one was an
413 SV-derived inner population giving rise to coronary ECs in the ventricular free wall, and
414 the other was a surface mesothelial population giving rise to epicardium, vascular
415 smooth muscle cells, and interstitial cells.
416

417 SV is a major source of coronary ECs in ventricular free wall

418 Prior to 2000, the origin of coronary ECs had been investigated using quail-chick
419 chimeras (co-transplantation of PEO and SV), retrovirus cell tracing, and fluorescent
420 dye labeling in avian species. These experiments are spatial labeling but not cell- or
421 tissue-specific labeling because the PEO contains at least two distinct compartments in
422 origin. Therefore, results from these experiments concluded that the PEO or PEO-
423 derived epicardium is the major source of coronary ECs (Reese *et al*. 2002). Our tissue-
424 specific labeling with quail-chick chimera and culture experiments showed that the SV
425 endothelium is the major source of coronary ECs in the ventricular free wall including
426 the coronary stems. The surface mesothelial cells of the PEO contributed to smooth
427 muscle cells but few of them to ECs. Our labeling experiment showed that the ratio of
428 the SV-derived population to the PEO-mesothelium-derived population in the
429 subepicardial QH1-positive cells was 9:1 (Fig. 7D). This ratio is consistent with mouse

lineage tracing experiments showing that 70–80% of coronary ECs in the ventricular free wall originates from the SV (Zhang *et al*. 2016). Mouse genetic approaches have shown that the main source of coronary ECs is the SV (Red-Horse *et al*. 2010; Wu *et al*. 2012; Tian *et al*. 2013; Chen *et al*. 2014; Zhang *et al*. 2016). The SV-derived ECs migrate through the subepicardial space, dedifferentiate and redifferentiate into venous and arterial ECs via unknown signaling possibly involving VEGF, Shh, FGF, and Ang1 (Red-Horse *et al*. 2010; Wu *et al*. 2012; Nakajima & Imanaka-Yoshida 2013; Tian *et al*. 2013; Tian *et al*. 2015). In our culture experiment, SV-derived cells had QH1 epitopes in 37% of cells after 48 hours in culture, subsequently they expressed QH1 in 80% of cells after 96 hours in culture. These results suggested that the SV-derived migrating cells initially dedifferentiated and then redifferentiated into ECs. Another possibility is that the cells migrating from the SV are endothelial progenitors, because the SV endothelium consists of heterogeneous populations (Arita *et al*. 2014). Our *in vivo* and *in vitro* observations suggested that SV ECs are incorporated into the developing PEO, spread over the ventricular surface together with the epicardium, and contribute to coronary vessels in the ventricular free wall including coronary stems.

Ventricular endocardium contributes mainly to the septal

448 **artery**

449 In our quail-chick chimeras, in which unlabeled quail SV with the PEO was co-
450 transplanted to endocardial-EGFP-labeled chick heart, EGFP-positive ECs were found
451 in the septal artery and coronary stem, whereas only a few EGFP-positive cells were
452 observed in the ventricular compact wall. In these chimeric hearts, QH1-
453 negative/EGFP-negative ECs were found in the septal arteries. This may be due to
454 methodological limitations of the Tol2-mediated EGFP expression system, in which the
455 transfection efficiency was low in the ventricular endocardium (Fig. S1B, E). In these
456 chimeric hearts, 90% of the coronary ECs in the ventricular compact wall were QH1-
457 positive cells originating from the transplanted quail SV (Fig. S4); therefore, the QH1-
458 negative/EGFP-negative coronary ECs in the ventricular septum were thought to
459 originate from the host ventricular endocardium rather than the host SV. This result was
460 consistent with that in mice, in which ventricular endocardium contributes to ventricular
461 septum, whereas SV contributes to ventricular free wall (Red-Horse *et al*. 2010; Tian *et*
462 *al*. 2013; Chen *et al*. 2014; Zhang *et al*. 2016). EGFP-positive ECs were also found in
463 the coronary artery stem. This observation was consistent with that in mice, in which the
464 ventricular endocardium contributes to the ventricular free wall of the ventral cardiac
465 base (Zhang *et al*. 2016). Another mouse model showed that the ventricular

endocardium is a major source of coronary arteries not only in the ventricular septum but also the ventricular free wall (Wu *et al.* 2012). The discrepancy between these two observations in the mouse models may be attributed to the genes that drive Cre-recombinase in target cells of interest, because the genes that drive Cre-recombination in cells are not exclusively cell-type specific (Tian *et al*. 2015; Zhang *et al*. 2016). In the neonatal mouse heart, ventricular endocardium differentiates into subendocardial coronary vasculature (Tian *et al*. 2014). Taken together with these observations, it appears plausible that the ventricular endocardium contributes to the coronary vessels in the ventricular septum as well as a minor part of the coronary stems.

Despite the methodological limitation, relatively low labeling efficiency of EGFP-Tol2 system, our results strongly suggested that 1) SV are the major source of coronary ECs of the ventricular free wall including the coronary stems; 2) the ventricular endocardium contributes mainly to septal coronary vessels; and 3) the surface mesothelium of the PEO is a minor source of ECs but is the source of coronary smooth muscles and interstitial cells.

Acknowledgments

Authors thank Ms Uoya for preparing the manuscript. This work was supported by

Japan Society for the Promotion of Science (JSPS) Grant-in-Aid for Scientific Research (C) 16K08450.

References

Ando K, Nakajima Y, Yamagishi T, Yamamoto S, Nakamura H. 2004. Development of proximal coronary arteries in quail embryonic heart: Multiple capillaries penetrating the aortic sinus fuse to form main coronary trunk. *Circ. Res*. **94**, 346-352.

Arita Y, Nakaoka Y, Matsunaga T, Kidoya H, Yamamizu K, Arima Y, Kataoka-Hashimoto T, Ikeoka K, Yasui T, Masaki T, Yamamoto K, Higuchi K, Park JS, Shirai M, Nishiyama K, Yamagishi H, Otsu K, Kurihara H, Minami T, Yamauchi-Takihara K, Koh GY, Mochizuki N, Takakura N, Sakata Y, Yamashita JK, Komuro I. 2014. Myocardium-derived angiopoietin-1 is essential for coronary vein formation in the developing heart. *Nat. Commun*. **5**, 4552.

Cano E, Carmona R, Ruiz-Villalba A, Rojas A, Chau YY, Wagner KD, Wagner N, Hastie ND, Muñoz-Chápuli R, Pérez-Pomares JM. 2016. Extracardiac septum transversum/proepicardial endothelial cells pattern embryonic coronary arterio-venous connections. *Proc. Natl Acad. Sci. U S A* **113**, 656-661.

Chen HI, Sharma B, Akerberg BN, Numi HJ, Kivela R, Saharinen P, Aghajanian H, McKay AS, Bogard PE, Chang AH, Jacobs AH, Epstein JA, Stankunas K, Alitalo K, Red-Horse K. 2014.

The sinus venosus contributes to coronary vasculature through vegfc-stimulated angiogenesis. *Development* **141**, 4500-4512.

Cossette S, Misra R. 2011. The identification of different endothelial cell populations within the mouse proepicardium. *Dev. Dyn*. **240**, 2344-2353.

Dettman RW, Denetclaw W, Jr. Ordahl CP, Bristow J. 1998. Common epicardial origin of coronary vascular smooth muscle, perivascular fibroblasts, and intermyocardial fibroblasts in the avian heart. *Dev. Biol*. **193**, 169-181.

Gittenberger-de Groot AC, Vrancken Peeters MP, Bergwerff M, Mentink MM, Poelmann RE. 2000. Epicardial outgrowth inhibition leads to compensatory mesothelial outflow tract collar and abnormal cardiac septation and coronary formation. *Circ. Res*. **87**, 969-971.

Guadix JA, Carmona R, Munoz-Chapuli R, Perez-Pomares JM. 2006. In vivo and in vitro analysis of the vasculogenic potential of avian proepicardial and epicardial cells. *Dev. Dyn*. **235**, 1014-1026.

Hamburger V, Hamilton HL. 1951. A series of normal stages in the development of the chick embryo. *J. Morphol*. **88**, 49-92.

Hiruma T, Hirakow R. 1989. Epicardial formation in embryonic chick heart: Computer-aided reconstruction, scanning, and transmission electron microscopic studies. *Am. J. Anat*. **184**, 129-138.

520 Kattan J, Dettman RW, Bristow J. 2004. Formation and remodeling of the coronary vascular bed
521 in the embryonic avian heart. *Dev. Dyn*. **230**, 34-43.
522 Katz TC, Singh MK, Degenhardt K, Rivera-Feliciano J, Johnson RL, Epstein JA, Tabin CJ. 2012.
523 Distinct compartments of the proepicardial organ give rise to coronary vascular endothelial
524 cells. *Dev. Cell* **22**, 639-650.
525 Kruithof BP, van Wijk B, Somi S, Kruithof-de Julio M, Perez Pomares JM, Weesie F, Wessels A,
526 Moorman AF, van den Hoff MJ. 2006. BMP and FGF regulate the differentiation of
527 multipotential pericardial mesoderm into the myocardial or epicardial lineage. *Dev. Biol*. **295**,
528 507-522.
529 Lindsay FE, Smith HJ. 1965. Coronary arteries of gallus domesticus. *Am. J. Anat*. **116**, 301-314.
530 Männer J. 1999. Does the subepicardial mesenchyme contribute myocardioblasts to the
531 myocardium of the chick embryo heart? A quail-chick chimera study tracing the fate of the
532 epicardial primordium. *Anat. Rec*. **255**, 212-226.
533 Mikawa T, Fischman DA. 1992. Retroviral analysis of cardiac morphogenesis: Discontinuous
534 formation of coronary vessels. *Proc. Natl Acad. Sci. U S A* **89**, 9504-9508.
535 Mikawa T, Gourdie R. 1996. Pericardial mesoderm generates a population of coronary smooth
536 muscle cells migrating into the heart along with ingrowth of the epicardial organ. *Dev.*
537 *Biol*. **174**, 221-232.

538 Nakajima Y, Imanaka-Yoshida K. 2013. New insights into the developmental mechanisms of
539 coronary vessels and epicardium. *Int. Rev. Cell Mol. Biol*. **303**, 263-317.
540 Niderla-Bielinska J, Gula G, Flaht-Zabost A, Jankowska-Steifer E, Czarnowska E, Radomska-
541 Lesniewska DM, Ciszek B, Ratajska A. 2015. 3-d reconstruction and multiple marker
542 analysis of mouse proepicardial endothelial cell population. *Microvasc. Res*. **102**, 54-69.
543 Pennisi DJ, Ballard VL, Mikawa T. 2003. Epicardium is required for the full rate of myocyte
544 proliferation and levels of expression of myocyte mitogenic factors fgf2 and its receptor,
545 fgfr-1, but not for transmural myocardial patterning in the embryonic chick heart. *Dev. Dyn*.
546 **228**, 161-172.
547 Pérez-Pomares JM, Carmona R, Gonzalez-Iriarte M, Atencia G, Wessels A, Munoz-Chapuli R.
548 2002. Origin of coronary endothelial cells from epicardial mesothelium in avian embryos.
549 *Int. J. Dev. Biol*. **46**, 1005-1013.
550 Poelmann RE, Gittenberger-de Groot AC, Mentink MM, Bokenkamp R, Hogers B. 1993.
551 Development of the cardiac coronary vascular endothelium, studied with antiendothelial
552 antibodies, in chicken-quail chimeras. *Circ. Res*. **73**, 559-568.
553 Red-Horse K, Ueno H, Weissman IL, Krasnow MA. 2010. Coronary arteries form by
554 developmental reprogramming of venous cells. *Nature* **464**, 549-553.
555 Reese DE, Mikawa T, Bader DM. 2002. Development of the coronary vessel system. *Circ. Res*.

91, 761-768.

Sato Y, Kasai T, Nakagawa S, Tanabe K, Watanabe T, Kawakami K, Takahashi Y. 2007. Stable integration and conditional expression of electroporated transgenes in chicken embryos. *Dev. Biol*. **305**, 616–624.

Shishibori T, Yamashita K, Bandoh J, Oyama Y, Kobayashi R. 1996. Presence of ca(2+)-sensitive and -insensitive sm22 alpha isoproteins in bovine aorta. *Biochem. Biophys. Res. Commun*. **229**, 225-230.

Takahashi M, Yamagishi T, Narematsu M, Kamimura T, Kai M, Nakajima Y. 2014. Epicardium is required for sarcomeric maturation and cardiomyocyte growth in the ventricular compact layer mediated by transforming growth factor beta and fibroblast growth factor before the onset of coronary circulation. *Congenit. Anom. (Kyoto)* **54**, 162-171.

Tian X, Hu T, Zhang H, He L, Huang X, Liu Q, Yu W, He L, Yang Z, Yan Y, Yang X, Zhong TP, Pu WT, Zhou B. 2014. De novo formation of a distinct coronary vascular population in neonatal heart. *Science* **345**, 90-94.

Tian X, Hu T, Zhang H, He L, Huang X, Liu Q, Yu W, He L, Yang Z, Zhang Z, Zhong TP, Yang X, Yang Z, Yan Y, Baldini A, Sun Y, Lu J, Schwartz RJ, Evans SM, Gittenberger-de Groot AC, Red-Horse K, Zhou B. 2013. Subepicardial endothelial cells invade the embryonic ventricle wall to form coronary arteries. *Cell Res*. **23**, 1075-1090.

574 Tian X, Pu WT, Zhou B. 2015. Cellular origin and developmental program of coronary
575 angiogenesis. *Circ. Res*. **116**, 515-530.
576 Vrancken Peeters MP, Gittenberger-de Groot AC, Mentink MM, Hungerford JE, Little CD,
577 Poelmann RE. 1997. Differences in development of coronary arteries and veins. *Cardiovasc.*
578 *Res*. **36**, 101-110.
579 Wilting J, Buttler K, Schulte I, Papoutsi M, Schweigerer L, Männer J. 2007. The proepicardium
580 delivers hemangioblasts but not lymphangioblasts to the developing heart. *Dev. Biol*. **305**,
581 451-459.
582 Wu B, Zhang Z, Lui W, Chen X, Wang Y, Chamberlain AA, Moreno-Rodriguez RA, Markwald
583 RR, O'Rourke BP, Sharp DJ, Zheng D, Lenz J, Baldwin HS, Chang CP, Zhou B. 2012.
584 Endocardial cells form the coronary arteries by angiogenesis through myocardial-
585 endocardial vegf signaling. *Cell* **151**, 1083-1096.
586 Yanagawa N, Sakabe M, Sakata H, Yamagishi T, Nakajima Y. 2011. Nodal signal is required for
587 morphogenetic movements of epiblast layer in the pre-streak chick blastoderm. *Dev.*
588 *Growth Differ*. **53**, 366-377.
589 Zhang H, Pu W, Li G, Huang X, He L, Tian X, Liu Q, Zhang L, Wu SM, Sucov HM, Zhou B.
590 2016. Endocardium minimally contributes to coronary endothelium in the embryonic
591 ventricular free walls. *Circ. Res*. **118**, 1880-1893.

Figure legends

Fig. 1. Quail-chick chimera. Four types of quail-chick chimera were prepared. (A) To trace the ECs of the SV, stage 16–17 quail SV with the PEO, in which ECs had been labeled with EGFP-Tol2 or DiI-LDL at stage 14, was orthotopically transplanted into PEO-cauterized host chick embryos at stage 17. (B) To trace the surface mesothelial cells of the PEO, stage 16–17 quail SV with the PEO, in which mesothelial cells had been labeled with EGFP-Tol2 or CFSE at stage 12–13, was orthotopically transplanted into PEO-cauterized host chick embryos at stage 17. (C) To trace both surface mesothelial cells of the PEO and ECs of the SV, stage 16–17 quail SV with the PEO, in which mesothelial cells had been labeled with CFSE at stage 12–13, followed by reincubation, and SV ECs labeling with DiI-LDL at stage 14, was orthotopically transplanted into PEO-cauterized host chick embryos at stage 17. (D) To trace the ventricular endocardium, unlabeled quail SV with the PEO was orthotopically transplanted into PEO-cauterized host chick hearts, in which the endocardium had been transfected with EGFP-Tol2 at stage 12.

Fig. 2. The PEO consists of at least two types of cells. (A) Stage 14–15 chick ECs were

610 labeled with DiI-LDL, then reincubated, and the PEO at stage 19 was stained with an
611 anti-WT1 antibody. Stage 19 PEO contained DiI-LDL-positive/WT1-negative cells
612 (white arrowheads) and DiI-LDL-negative/WT1-positive cells (yellow arrowheads). (B)
613 Stage 13 chick PEO mesothelial cells were labeled with CFSE, then reincubated, and
614 stage 16 PEO was stained an anti-WT1 antibody. CFSE-positive/WT1-positive cells
615 were observed on the surface of the PEO (yellow arrowheads), whereas CFSE-
616 negative/WT1-negative cells were present within the PEO (white arrowheads). At,
617 atrium; SV, sinus venosus, V, ventricle; scale bar, 25 μm
618
619 **Fig. 3.** SV ECs contribute to coronary vessels. Stage 16–17 quail SV with the PEO, in
620 which ECs had been labeled with EGFP-Tol2 at stage 14, was orthotopically
621 transplanted into PEO-cauterized host chick embryos at stage 17. After reincubation, the
622 hearts of chimeric embryos were stained with anti-QH1 or anti-smooth muscle α-actin
623 (SMA) antibodies. (A) At stage 23, QH1-positive cells, some of which had EGFP, were
624 observed in the subepicardial and myocardial layer (arrowheads). (B, C) At stage 29,
625 QH1-positive cells, some of which had EGFP, were observed as endothelial strands or
626 vessel-like structures in the ventricular free wall (arrowheads). (D, E) At stage 34, QH1-
627 positive and EGFP-positive cells were observed in not only SMA-positive coronary

628 stem (arrowheads) but also the SMA-negative cardiac vein (arrows). Note that panels D
629 and E are daughter sections. Ao, ascending aorta; LA, left atrium; LV, left ventricle, PA,
630 pulmonary trunk; scale bar, 100 μm (A4, B4, C4, D, E); 50 μm (B1–3); 25 μm (A1–3,
631 C1–3).
632
633 **Fig. 4.** Cultured SV ECs migrate through the PEO and maintain endothelial lineage.
634 PEOs with SV, in which ECs had been labeled with DiI-LDL, were cultured. Cultures
635 were fixed and stained with an anti-QH1 antibody and observed using a confocal
636 microscope. (A-F) DiI-LDL-labeled ECs of SV migrated through the PEO and
637 expanded on the culture dish. High magnification (white box in A-C) showed that some
638 of DiI-LDL-positive cells had QH1 immunoreactivity (arrowheads). Note that the
639 yellow broken line indicates the eggshell membrane inserted into the SV. (G-L) DiI-
640 LDL/QH1-positive cells appeared as mesenchyme-like appearance after 48 hours in
641 culture, whereas these cells showed a cobblestone appearance after 72–96 hours. (M)
642 Percentage incidence of QH1-positive cells in DiI-LDL-positive cells. 25–90 cells were
643 examined in each explant. *, $P<0.05$ (Mann-Whitney *U* test after Bonferroni
644 correction); NS, not significant; n, number of explants examined. Scale bar, 80 μm (A-
645 C); 20 μm (others).

Fig. 5. Surface mesothelial cells of the PEO mostly contributed coronary smooth muscles and few to ECs. Quail SV with the PEO, in which mesothelial cells had been labeled with EGFP-Tol2 was orthotopically transplanted into host chick embryos. (A) At stage 23, EGFP-positive cells were observed in the subepicardial space and some EGFP-positive cells had QH1 immunoreactivity (arrowheads). (B) At stage 29, a few EGFP-positive cells were incorporated into QH1-positive vessel-like structures (arrowheads). (C) In stage 34 hearts, EGFP-positive cells were distributed in the epicardium, subepicardial (double-headed arrow), and myocardial layer. EGFP-positive cells were incorporated into the tunica media of coronary arteries (arrows). (D) A few EGFP-positive cells were observed in the QH1-positive coronary endothelium (arrowheads). Note that panel D is a daughter section of panel C; solid arrowheads indicate coronary artery and open arrowheads cardiac vein. AVC, atrioventricular canal; LA, left atrium; OFT, outflow tract; PA, pulmonary artery; RA, right atrium; qSV, quail sinus venosus; Scale bar, 25 μm (A1–3, B1–3, C1–3, D1–3); 100 μm (A4); 250 μm (B4, C4, D4).

Fig. 6. Cultured PEO mesothelial cells differentiated into a smooth muscle phenotype but a few differentiated into ECs. Chick or quail PEOs, in which mesothelial cells were labeled with CFSE, were cultured and stained with antibodies to detect smooth muscle markers or QH1. (A-C) After 72 hours in culture, almost all the cells possessed CFSE, and these CFSE-positive cells expressed smooth muscle markers. Approximately 5% (4.7 ± 4.2%) of CFSE-positive cells expressed QH1. n, number of explants examined. (D-K) Some CFSE-positive cells generated vessel-like strands labeled with QH1 (arrowheads) and luminal structures were observed using confocal microscopic three-dimensional reconstruction (indicated broken line in H). Scale bar, 20 μm (A, B, E–K); 50 μm (D).

Fig. 7. QH1-positive subepicardial cells are mainly derived from the SV. Quail PEO with SV, in which ECs and surface mesothelium had been labeled with DiI-LDL and CFSE, respectively, was orthotopically transplanted into PEO-cauterized chick embryos at stage 17, reincubated and stage 24 (E4) hearts were stained with QH1 antibody. (A) CFSE-positive cells were distributed mainly in the epicardium (double-headed arrow), whereas DiI-LDL-positive cells were in the subepicardial space and myocardium. (B, C) QH1 staining showed that QH1-positive cells with DiI-LDL (arrowheads) were more

predominant than those with CFSE (arrows). (D) To examine the significance of DiI-LDL-positive cells in QH1-stained cells, we made type A and type B chimeras (Fig. 1). At stage 24 (E4), QH1 staining was performed, and the percentage of DiI-LDL- or CFSE-positive cells in the QH1-positive cells were counted manually in region where the PEO attached to the ventricle. In QH1-stained cells, percentage of DiI-LDL-positive cells (44.5 ± 6.1%) was significantly higher than that of CFSE-positive cells (5.1 ± 0.9%) (P=0.0495, Mann-Whitney U test). n, number of embryos examined; V, ventricle; scale bar, 25 μm.

Fig. 8. Ventricular endocardium contributes to septal artery. Unlabeled quail PEO with SV was orthotopically transplanted into PEO-cauterized chick hearts, in which the ventricular endocardium had been transfected with EGFP-Tol2. (A, B) In stage 35 (E9) chimeric hearts, QH1-positive cells were distributed in a compact myocardial layer of left and right ventricular free wall. EGFP-positive cells were observed in the endocardium of the trabecular layer. (C) In the dorsal ventricular septum, QH1-positive cells were densely distributed, whereas EGFP-positive cells were observed in the middle to ventral aspect of the septum (arrowheads). (D, E) Coronary stems had an SMA-positive medial layer. In the stems EGFP-positive ECs were sparse (arrowhead),

699 but QH1-positive ECs were predominant (arrows). (F, G) Septal artery had SMA-
700 positive medial layer. Both EGFP- (arrowheads) and QH1-positive (arrows) ECs were
701 observed in dorsal septal arteries. Ao, aorta; LA, left atrium; LV, left ventricle; PA,
702 pulmonary artery; RA, right atrium; RV, right ventricle; Scale bar, 250 μm (A4, B4, C4,
703 E4, F4); 100 μm (A1–3, B1–3, C1–3, D4, G4); 25 μm (D1–3, E1–3, F1–3, G1–3).
704
705 **Fig. 9.** Endothelial fractions in coronary stem and septal artery. Quail PEO with SV was
706 orthotopically transplanted into PEO-cauterized chick hearts, in which the ventricular
707 endocardium had been transfected with EGFP-Tol2. At stage 35, chimeric hearts were
708 stained with QH1, and the percentage of QH1- or EGFP-positive ECs was counted
709 manually in the coronary endothelium, in which the vascular segment was more than
710 100 μm in histological sections. *, $P<0.05$; **, $P<0.01$ (Mann-Whitney *U* test after
711 Bonferroni correction); NS, not significant; Red bar, % of QH1-positive ECs; green,
712 EGFP-positive ECs; gray, unlabeled ECs; n, number of endothelial segments examined.
713
714 **Fig. 10.** Schematic representations of the sources of coronary ECs. (A) Ventricular
715 septum is shown from the right ventricle (right ventricular free wall is removed). (B)
716 Cross-section of the ventricles. In the ventricular free wall, coronary ECs originate from

717 SV endothelium (approximately 80%) and PEO surface mesothelium. In the ventricular
718 septum, coronary ECs originate from the ventricular endocardium (approximately 70-
719 80%) and SV endothelium in the middle to ventral region, while SV endothelium and
720 the ventricular endocardium evenly contribute to the dorsal region. Ao, ascending aorta;
721 LV, left ventricle; PA, pulmonary artery; RV, right ventricle; TV, tricuspid valve.
722

723 Legends for supporting information

724 **Fig. S1.** Fluorescently labeled ECs and mesothelial cells of the PEO. (A) Stage 19 heart.
725 ECs in the SV, atrioventricular canal and ventricle (V) as well as endocardium-derived
726 cushion mesenchymal cells were labeled with DiI-LDL, which had been injected into
727 the peripheral vitelline vein at stage 15. ECs and endocardium-derived cushion
728 mesenchymal cells were stained with an anti-QH1 antibody. (B) Stage 18 heart. ECs in
729 the SV, atrioventricular canal and ventricle were labeled with EGFP-Tol2, which had
730 been transfected at stage 12. (C) Stage 14 PEO. Surface mesothelial cells were labeled
731 with CFSE, which had been injected into the pericardial cavity at stage 13. (D) Stage 16
732 PEO and stage 19 heart. WT1-positive mesothelial cells and epicardial cells expressed
733 EGFP, which had been transfected at stage 13. (E) Labeling efficiency of EGFP-tol2
734 system *in vivo*. In tissue sections, percentages of EGFP-positive cells in the

735 endocardium, PEO surface cells and epicardium was manually calculated. The labeling
736 efficiencies were 15.4 ± 4.2% in stage 18 endocardium/SV endothelium (n=3), 12 ±
737 1.1% in stage 35 (E9) endocardium (n=3), 7.3 ± 0.8% in stage 16 PEO surface
738 mesothelium (n=3), and 24% in stage 19 epicardium (n=1). PEO, proepicardial organ;
739 SV, sinus venosus; V, ventricle.
740
741 **Fig. S2.** SV endothelial cells expressed Slug and contribute to PEO-core mesenchyme.
742 (A) Stage 16-17 chick PEO was stained with anti-Slug antibody (clone 62.1E6, mouse
743 IgG1, Developmental Studies Hybridoma Bank). SV ECs and adjacent PEO-core
744 mesenchymal cells expressed an epithelial-to-mesenchymal transition marker, Slug. (B)
745 PEO-core mesenchymal cells were labeled with DiI-LDL, which had been injected into
746 the peripheral vitelline vein at stage 14 (arrows). (C) In tissue sections, the percentage
747 of DiI-LDL-positive cells in PEO-core mesenchyme (76 ± 12%) was greater than that of
748 DiI-LDL-negative cells (24 ± 12%, $P = 0.004$, paired *t*-test). n, number of PEO
749 examined; PEO, proepicardial organ; SV, sinus venosus; V, ventricle.
750
751 **Fig. S3.** Surface mesothelial cells of the PEO contributed mainly to the coronary
752 smooth muscle cells.

753 Type B chimera, in which surface mesothelial cells were labeled with EGFP. After
754 reincubation, stage 34 (E8) heart sections were stained with an anti-SMA or anti-QH1
755 antibody. Number of SMA- (or QH1)/EGFP-positive cells was manually counted in
756 tissue sections (at least 5sections were examined in each heart, n=2). The percentage of
757 SMA- (or QH1)-positive cells in EGFP-positive cells was calculated and compared. *,
758 $P<0.05$ (Mann-Whitney *U* test).
759
760 **Fig. S4.** Coronary ECs in the ventricular free wall of the chimeric heart originated from
761 transplanted quail SV. Unlabeled quail SV with PEO was orthotopically transplanted
762 into a PEO-cauterized chick heart and reincubated. At stage 38 (E12), FITC-conjugated
763 lectin (LCA, *Lens culinaris* agglutinin) was injected into the ascending aorta to
764 visualize coronary ECs. Hearts were fixed in 4% paraformaldehyde/PBS and cryostat
765 sections were stained with an anti-QH1 antibody. The percentage of QH1-positive ECs
766 in LCA-stained ECs (170 - 400 LCA-positive ECs in 5 sections were manually counted
767 in each region) was calculated. In the left or right ventricular free wall, 90% of LCA-
768 positive ECs was stained with QH1. In the ventricular septum, 58% of LCA-positive
769 ECs was stained with QH1 in the dorsal region, while 30% in the medial region and
770 28% in the ventral region. LV, left ventricle; RV, right ventricle.

Table S1. Number of chimera hearts examined. Number of chimeric hearts in each experiment was summarized. Details of each chimera were shown in Fig. 1.

Fig. 1

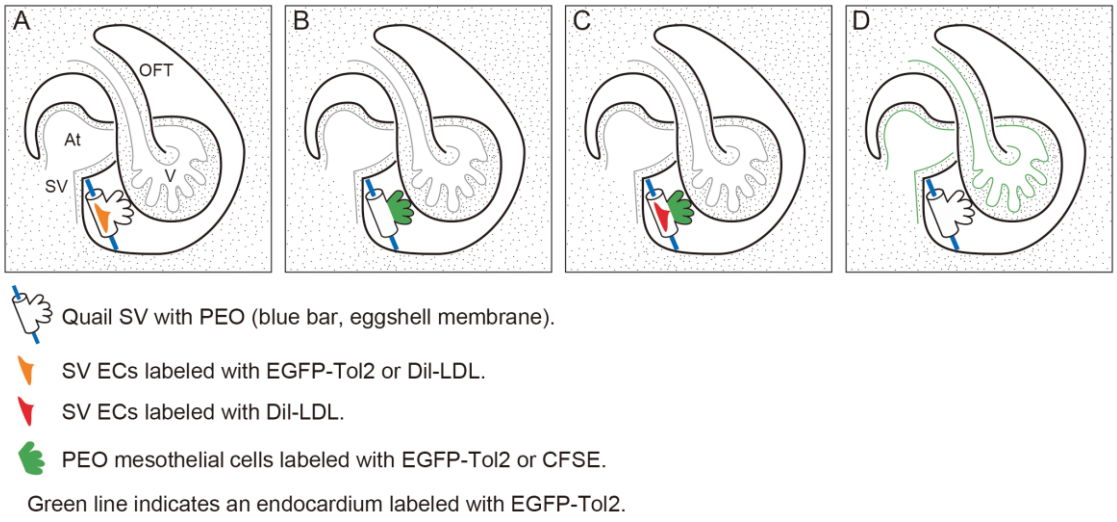

Fig. 2

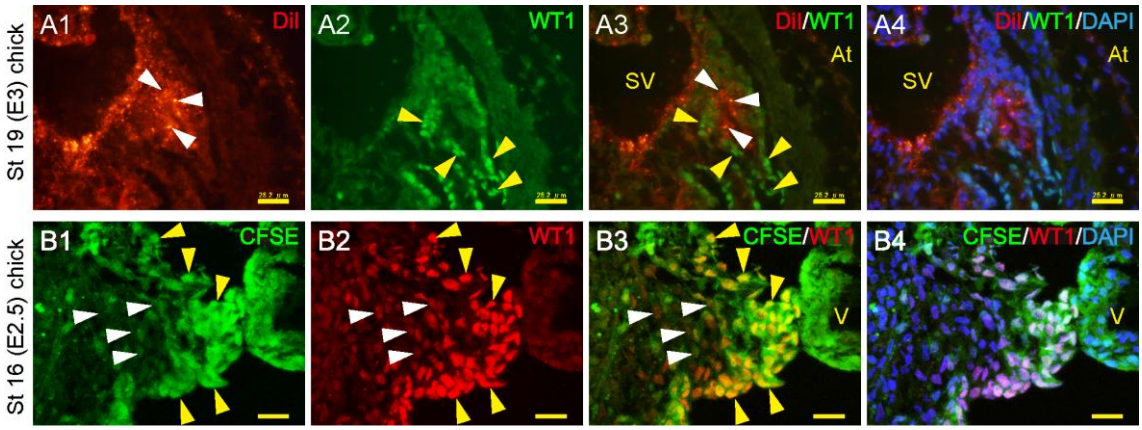
St 19 (E3) chick
St 16 (E2.5) chick
A1
DiI
A2
WT1
A3
DiI/WT1
SV
At
A4
DiI/WT1/DAPI
SV
At
B1
CFSE
B2
WT1
B3
CFSE/WT1
V
B4
CFSE/WT1/DAPI
V

Fig. 3

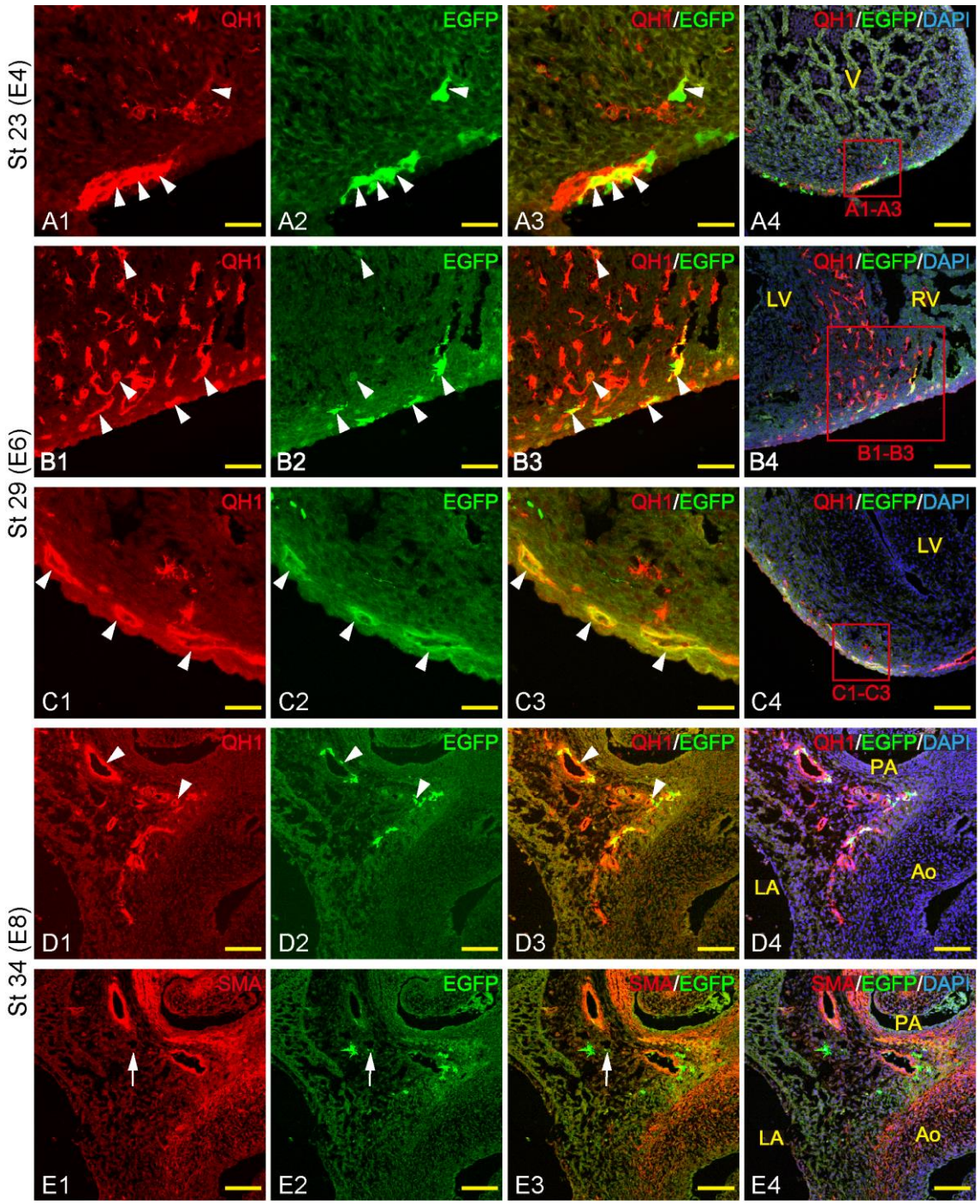

785

786

787

788 **Fig. 4**

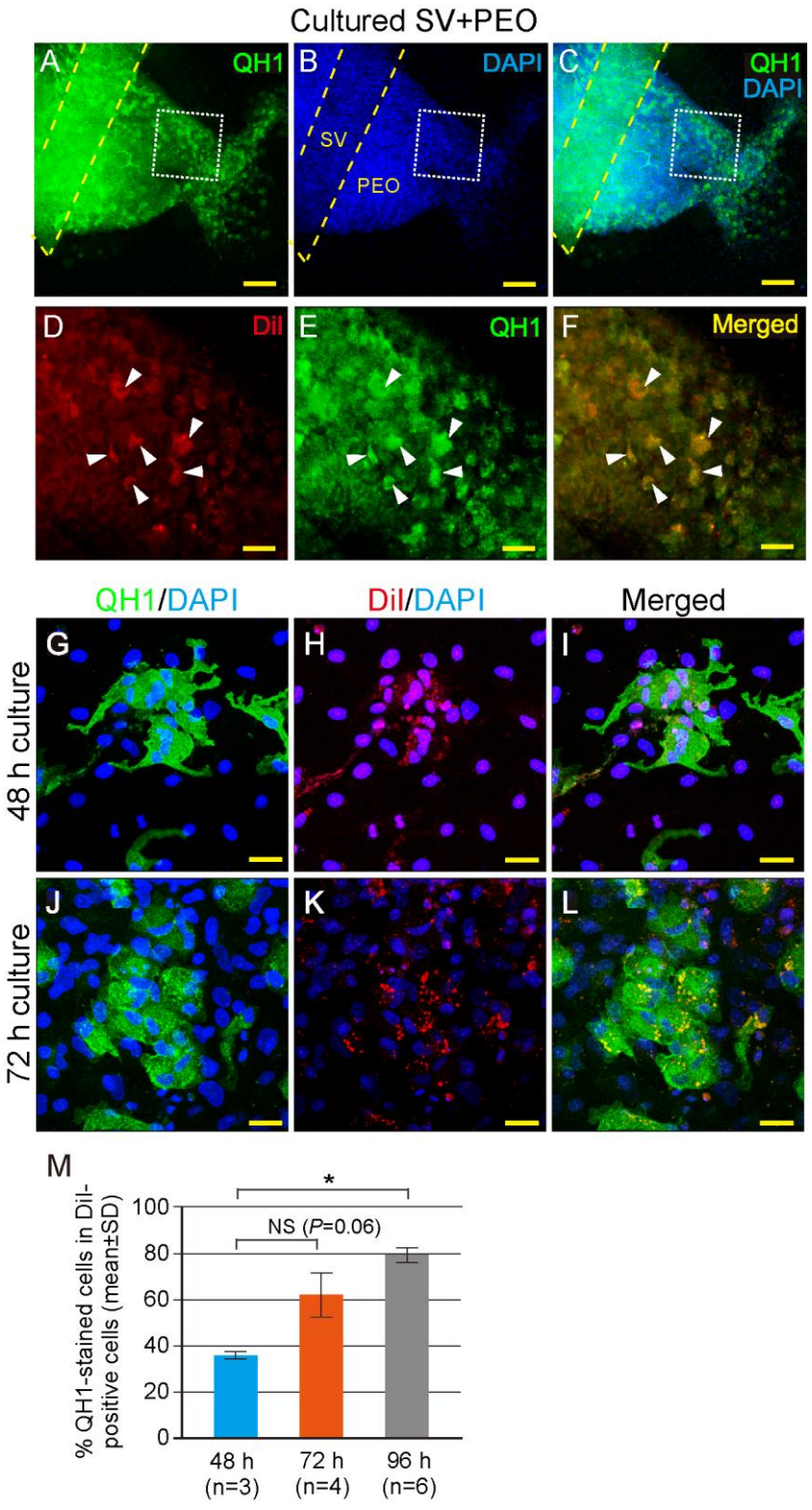
Cultured SV+PEO
A
QH1
B
DAPI
SV
PEO
C
QH1
DAPI
D
DiI
E
QH1
F
Merged
QH1/DAPI
DiI/DAPI
Merged
48 h culture
G
H
I
72 h culture
J
K
L
M
% QH1-stained cells in DiI-positive cells (mean±SD)
100
80
60
40
20
0
*
NS (P=0.06)
48 h
(n=3)
72 h
(n=4)
96 h
(n=6)

789

790

791

Fig. 5

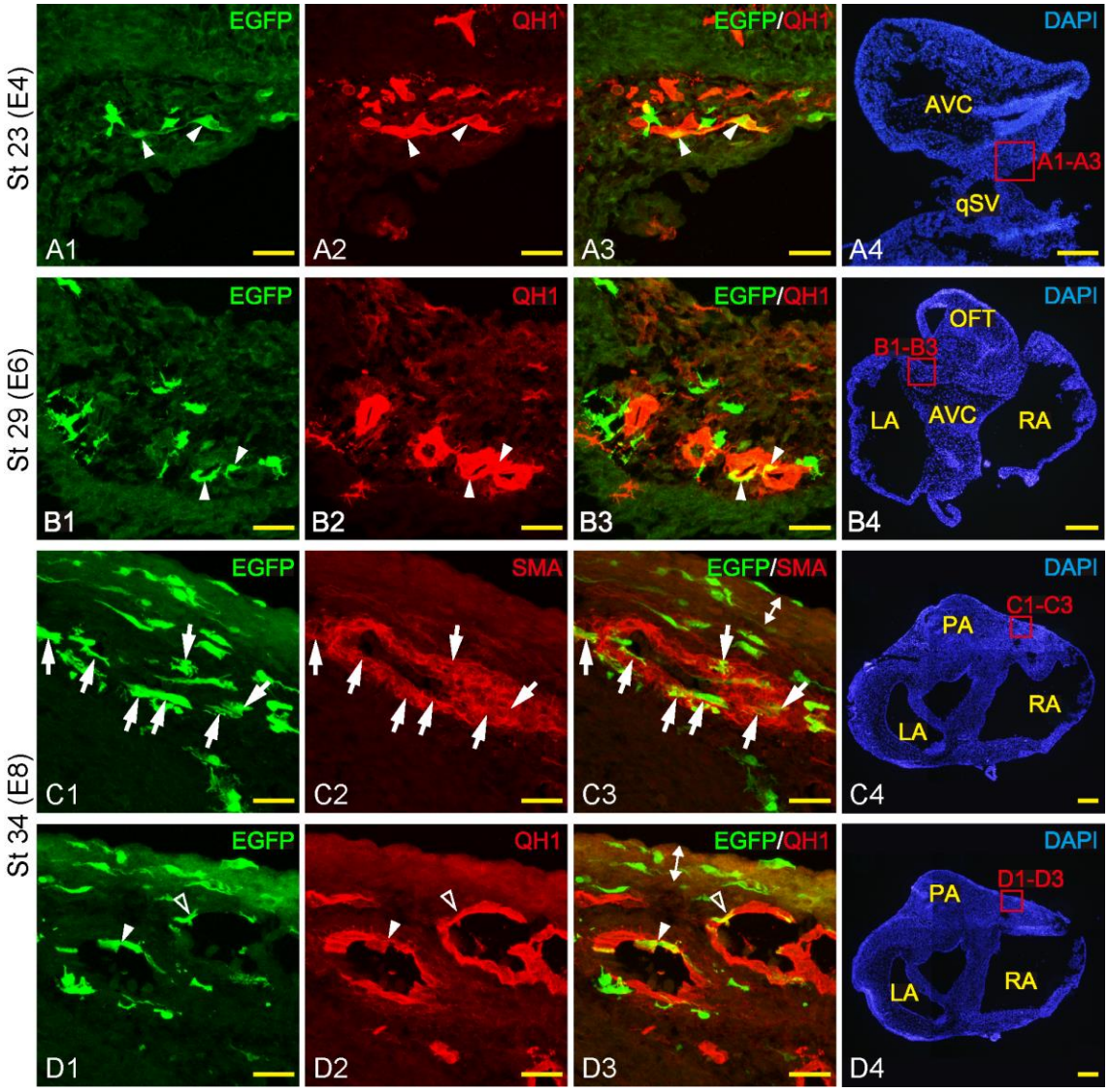
St 23 (E4)
St 29 (E6)
St 34 (E8)
EGFP
QH1
EGFP/QH1
DAPI
SMA
EGFP/SMA
AVC
A1-A3
qSV
OFT
B1-B3
LA
RA
PA
C1-C3
D1-D3
A1
A2
A3
A4
B1
B2
B3
B4
C1
C2
C3
C4
D1
D2
D3
D4

Fig. 6

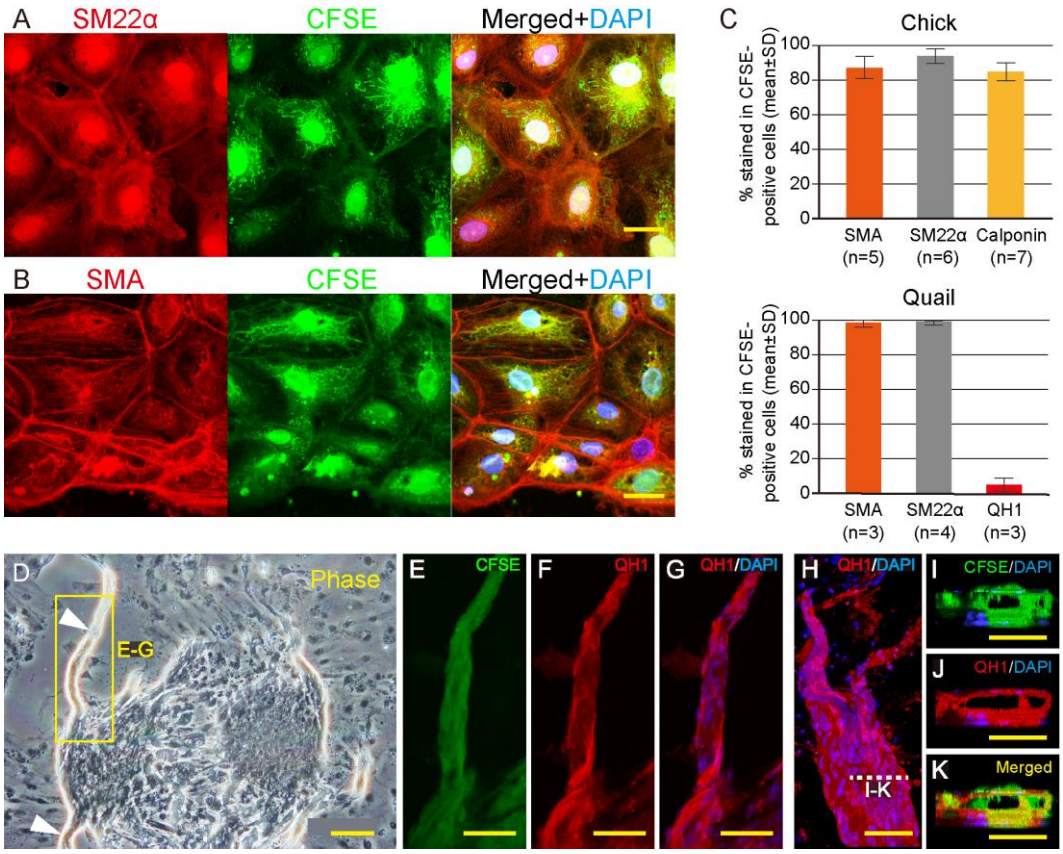

797

798

799

800 **Fig. 7**

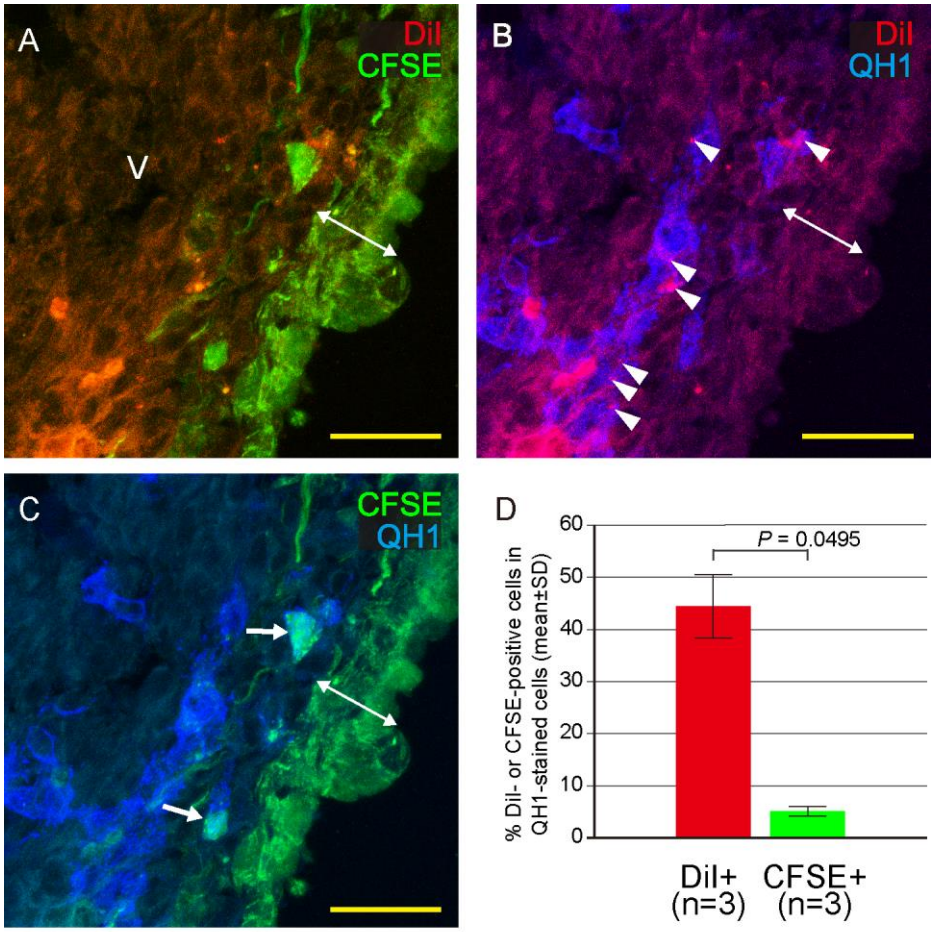

801

802

803

804 **Fig. 8**

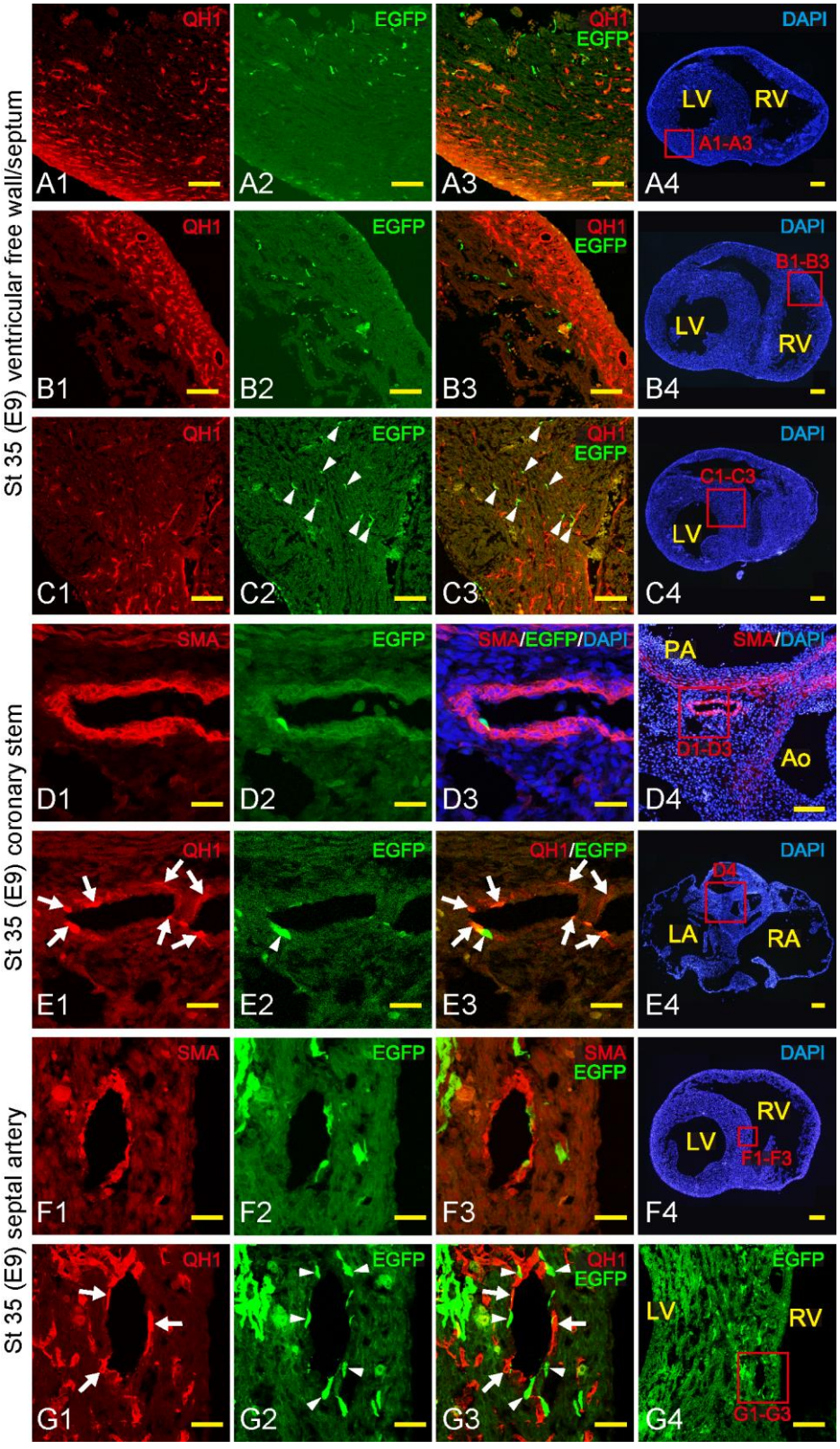
St 35 (E9) ventricular free wall/septum
St 35 (E9) coronary stem
St 35 (E9) septal artery
QH1
EGFP
DAPI
SMA
SMA/EGFP/DAPI
SMA/DAPI
QH1/EGFP
SMA
EGFP
LV
RV
A1-A3
B1-B3
C1-C3
PA
D1-D3
Ao
LA
RA
F1-F3
G1-G3
A1
A2
A3
A4
B1
B2
B3
B4
C1
C2
C3
C4
D1
D2
D3
D4
E1
E2
E3
E4
F1
F2
F3
F4
G1
G2
G3
G4

805

806

807

808 **Fig. 9**

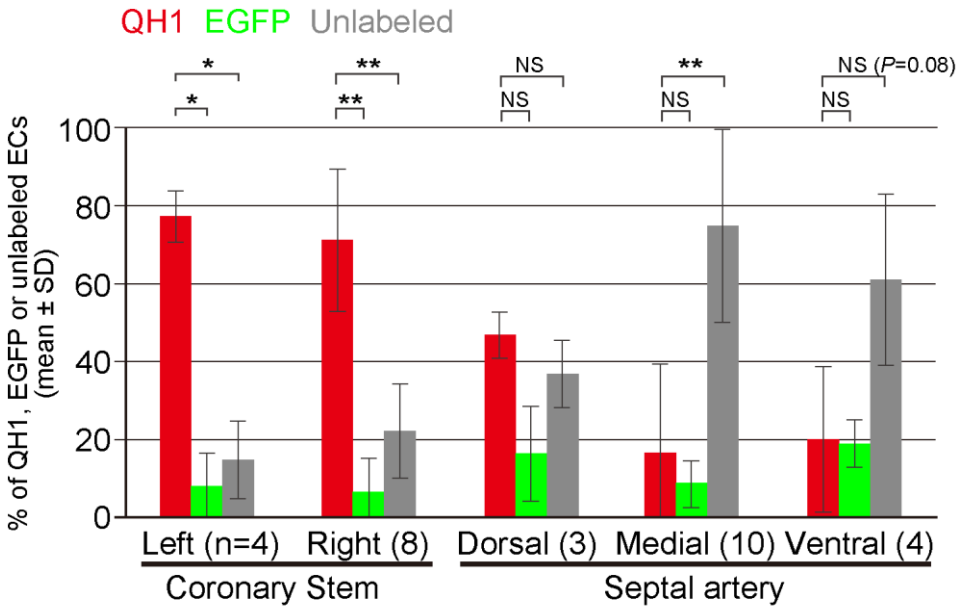

809

810

811

812 **Fig. 10**

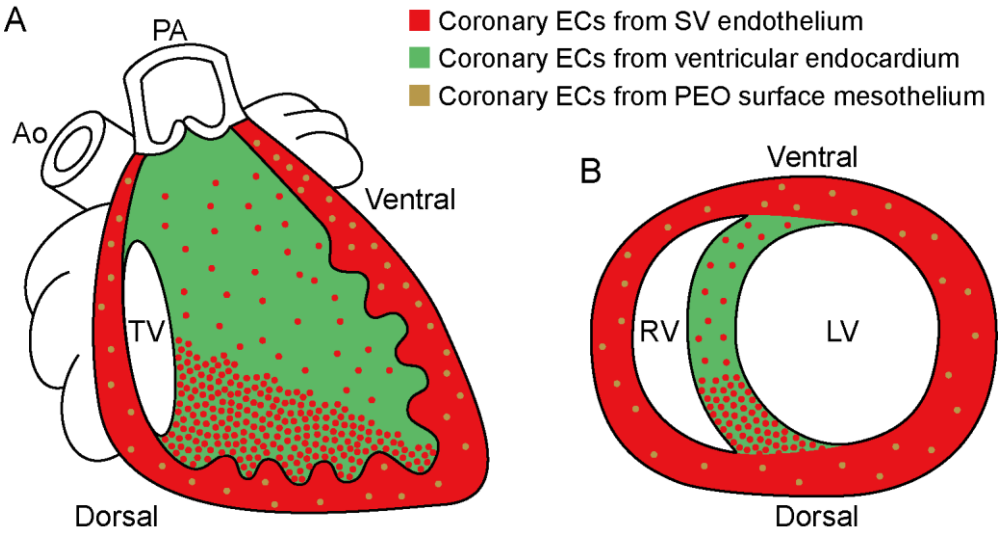

813

814

Fig. S1

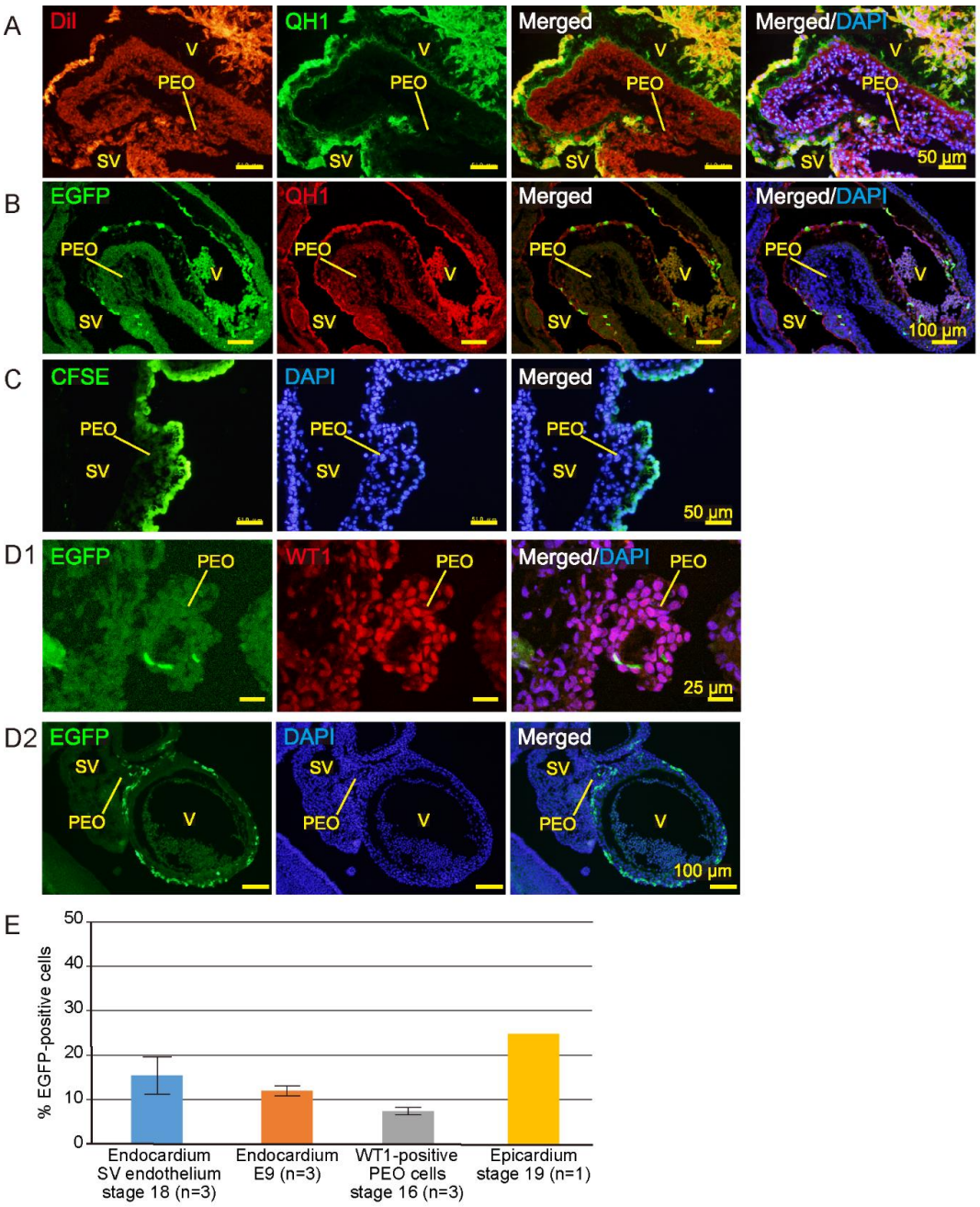

Fig. S1. Fluorescently labeled ECs and mesothelial cells of the PEO. (A) Stage 19 heart. ECs in the SV, atrioventricular canal and ventricle (V) as well as endocardium-derived cushion mesenchymal cells were labeled with DiI-LDL, which had been injected into the peripheral vitelline vein at stage 15. ECs and endocardium-derived cushion mesenchymal cells were stained with an anti-QH1 antibody. (B) Stage 18 heart. ECs in the SV, atrioventricular canal and ventricle were labeled with EGFP-Tol2, which had been transfected at stage 12. (C) Stage 14 PEO. Surface mesothelial cells were labeled with CFSE, which had been injected into the pericardial cavity at stage 13. (D) Stage 16 PEO and stage 19 heart. WT1-positive mesothelial cells and epicardial cells expressed EGFP, which had

been transfected at stage 13. (E) Labeling efficiency of EGFP-tol2 system *in vivo*. In tissue sections, percentages of EGFP-positive cells in the endocardium, PEO surface cells and epicardium was manually calculated. The labeling efficiencies were 15.4 ± 4.2% in stage 18 endocardium/SV endothelium (n=3), 12 ± 1.1% in stage 35 (E9) endocardium (n=3), 7.3 ± 0.8% in stage 16 PEO surface mesothelium (n=3), and 24% in stage 19 epicardium (n=1). PEO, proepicardial organ; SV, sinus venosus; V, ventricle.

Fig. S2

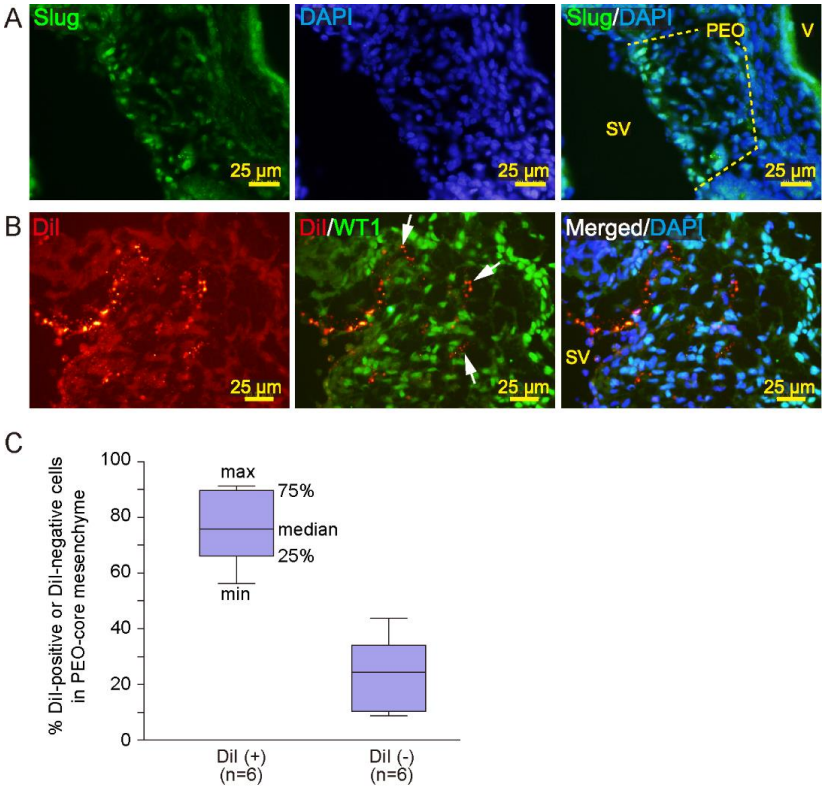

Fig. S2. SV endothelial cells expressed Slug and contribute to PEO-core mesenchyme. (A) Stage 16-17 chick PEO was stained with anti-Slug antibody (clone 62.1E6, mouse IgG1, Developmental Studies Hybridoma Bank). SV ECs and adjacent PEO-core mesenchymal cells expressed an epithelial-to-mesenchymal transition marker, Slug. (B) PEO-core mesenchymal cells were labeled with DiI-LDL, which had been injected into the peripheral vitelline vein at stage 14 (arrows). (C) In tissue sections, the percentage of DiI-LDL-positive cells in PEO-core mesenchyme (76 ± 12%) was greater than that of DiI-LDL-negative cells (24 ± 12%, $P = 0.004$, paired *t*-test). n, number of PEO examined; PEO, proepicardial organ; SV, sinus venosus; V, ventricle.

Fig. S3

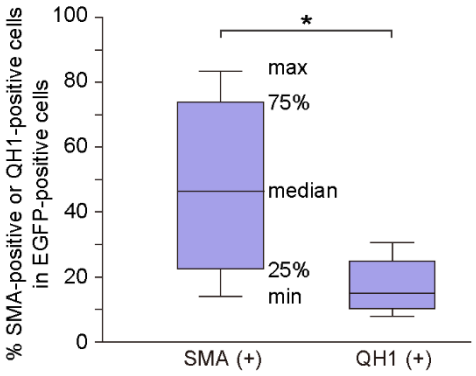

Fig. S3. Surface mesothelial cells of the PEO contributed mainly to the coronary smooth muscle cells.Type B chimera, in which surface mesothelial cells were labeled with EGFP. After reincubation, stage 34 (E8) heart sections were stained with an anti-SMA or anti-QH1 antibody. Number of SMA- (or QH1)/EGFP-positive cells was manually counted in tissue sections (at least 5sections were examined in each heart, n=2). The percentage of SMA- (or QH1)-positive cells in EGFP-positive cells was calculated and compared. *, $P<0.05$ (Mann-Whitney *U* test).

Fig. S4

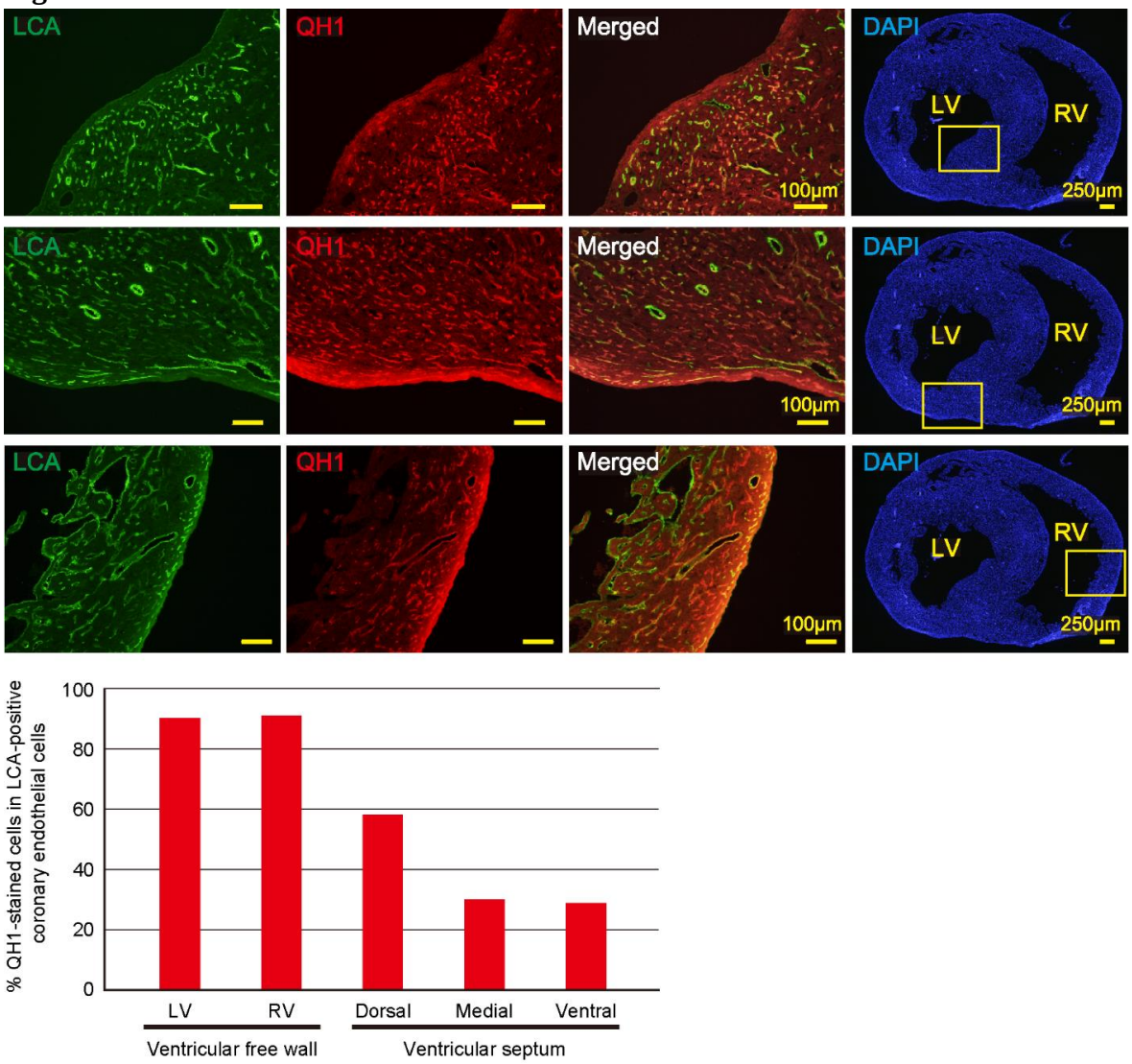

Fig. S4. Coronary ECs in the ventricular free wall of the chimeric heart originated from transplanted quail SV. Unlabeled quail SV with PEO was orthotopically transplanted into a PEO-cauterized chick heart and reincubated. At stage 38 (E12), FITC-conjugated lectin (LCA, *Lens culinaris* agglutinin) was injected into the ascending aorta to visualize coronary ECs. Hearts were fixed in 4% paraformaldehyde/PBS and cryostat sections were stained with an anti-QH1 antibody. The percentage of QH1-positive ECs in LCA-stained ECs (170 - 400 LCA-positive ECs in 5 sections were manually counted in each region) was calculated. In the left or right ventricular free wall, 90% of LCA-positive ECs was stained with QH1. In the ventricular septum, 58% of LCA-positive ECs was stained with QH1 in the dorsal region, while 30% in the medial region and 28% in the ventral region. LV, left ventricle; RV, right ventricle.

Table S1

Chimera A (shown in Fig 3)	E4	E5		E6	E7	E8	Total
EGFP	4			3		2	9
DiI-LDL	6	4		3	2	2	17
Chimera B (Fig 5)	E4	E5		E6	E7	E8	
EGFP	1			2		2	5
CFSE	5	3		3	2	4	17
Chimera C (Fig 7)	E4						
DiI-LDL/CFSE	7						7
Chimera A (Fig 7)	E4						
DiI-LDL	3						3
Chimera B (Fig 7)	E4						
CFSE	3						3
Chimera D (Fig 8)	E9						
EGFP	3						3

Table S1. Number of chimera hearts examined. Number of chimeric hearts in each experiment was summarized. Details of each chimera were shown in Fig. 1..